

## RESEARCH ARTICLE

# Mechanical Behavior of Hybrid Laminated Nano Composite Containing Equal Numbers of Glass and Carbon Fiber Plies

Ava A.K. Mohammed\*, Gailan Ismail Hassan and Younis Khalid Khdir

Department of Technical Mechanical and Energy Engineering, Erbil Technical Engineering College, Erbil Polytechnic University, 44001 Erbil, Iraq

**ABSTRACT** - Hybrid fiber reinforced polymer with nanofiller composite was introduced into a lot of industries due to its extreme mechanical properties in comparison with non-hybrid material. In this investigation, cross and quasi-fiber laminated epoxy composites with and without nano Al<sub>2</sub>O<sub>3</sub> were fabricated using Vacuum Assisted Resine Infusion Method and Ultrasonic Dual Mixing Method. In general, the results of mechanical properties indicated that the addition of 2% nano Al<sub>2</sub>O<sub>3</sub> enhances the tensile and flexural properties. Cross number 2 with nano Al<sub>2</sub>O<sub>3</sub> laminate had the maximum tensile strength 628 MPa and maximum tensile strain of 1.74%, while cross number 1 with nano Al<sub>2</sub>O<sub>3</sub> laminate had the maximum tensile modulus of 37.756 GPa in the cross group. In the quasi group, quasi number 2 with nano Al<sub>2</sub>O<sub>3</sub> had the maximum tensile strength, maximum tensile strain, and maximum tensile modulus, equal to 294 MPa, 1.98%, and 16.409 GPa, respectively. Regarding the flexural properties, cross number 1 with nano Al<sub>2</sub>O<sub>3</sub> laminate had a maximum flexural strength of 708.2 MPa and maximum flexural strain of 2.027%, while cross number 2 with nano Al<sub>2</sub>O<sub>3</sub> laminate had a maximum flexural modulus of 38.73 GPa in the cross group. On the other hand, quasi number 1 with nano Al<sub>2</sub>O<sub>3</sub> laminate had the maximum flexural strength, maximum flexural strain, and maximum flexural modulus equal to 596 MPa, 2.424%, and 29.2 GPa, respectively in the quasi group. The internal structures of the failure laminated composites through scanning electronic microscopy confirm that the adhesion between fibers and matrix is good.

## ARTICLE HISTORY

Received : 18<sup>th</sup> July 2022  
 Revised : 24<sup>th</sup> Nov 2022  
 Accepted : 20<sup>th</sup> March 2023  
 Published : 30<sup>th</sup> June 2023

## KEYWORDS

Glass/carbon hybrid;  
 Nano-Al<sub>2</sub>O<sub>3</sub>;  
 VARIM;  
 Cross laminates;  
 Quasi laminates

## 1.0 INTRODUCTION

High specific strength (strength to density ratio) and high specific stiffness (modulus to density ratio) connected with lightweight and enhancement in corrosion, wear and fatigue resistance are the essential reason to replace the conventional metal by fiber reinforced polymer laminated composite (FRP) in structural applications like aerospace, automobile and turbine blades [1]. The most common fibers used in industrial applications are carbon and glass. The use of carbon fiber in structural parts alone is unsuitable, despite its high strength and modulus due to its low strain-to-failure. To overcome the disadvantages of carbon, glass fiber was added to it, where the latter has low strength and modulus, but the strain to failure is high [2]. Hybridizing carbon with glass and vice versa is one of the important ways to eliminate the disadvantage of the fibers and to reduce the weight and cost. As a result of the contrastive coefficient of thermal expansions of carbon fiber and glass fiber, the stress-strain curve of CFRP after hybridization moves to higher strain-to-failure because of the formation of residual compressive strain in carbon fiber following the curing process [3, 14]. The objective of this work is to prevent the brittle fracture of carbon fiber laminated epoxy composite by adding some ductility to it through the addition of glass fiber to it. In order to transfer the load completely from matrix to the fiber, nano Al<sub>2</sub>O<sub>3</sub> was added to the epoxy resin, which led to an increase in the mechanical properties of the hybrid composite.

In this study, the first section is a very brief introduction to the fiber hybridization idea, followed by a literature review. Then, experimental work with all subdivisions alongside results and discussions are explained, and finally, a concise conclusion is written.

### 1.1 Glass: Carbon Fiber Hybrid Composite

It is possible to obtain hybrid composite materials in several ways and then find their mechanical properties related to the previous works. Researchers [4, 5, 6, 7, 8] investigated the influence of stacking sequence and the hybrid ratio of woven glass and carbon on the mechanical properties (strength and stiffness) of inter-ply hybrid FRP laminated composites. When the glass: carbon (G: C) hybrid ratio is 1:1, the balance mechanical properties were evaluated either by putting the carbon layers at the surface or by putting different layer types alternatively [4]. In [5, 6, 7, 8], researchers fabricated ten layers of carbon and glass laminated composites. The [GCGGC]s has tensile and flexural strength more than [CGGCG], while [CGGCG]s has higher tensile and flexural modulus by 20% and 36.2%, respectively, as compared to [GCGGC] [5]. Tensile strength, strains, and flexural extension of [G3C2]s were higher by 11.5%, 23%, and 39% than [C2G3]s, but flexural strength and modulus of [C2G3]s were higher by 23% and 64% than [G3C2]s [6]. The tensile and

flexural strength of [G2C2G]<sub>s</sub> were higher by 10.5% and 2.5%, respectively, than that of [CG3C]<sub>s</sub>, but the tensile strain and flexural extension of [G2C2G]<sub>s</sub> was 17.5% and 35.8% more than that of [CG3C]<sub>s</sub>, respectively [7]. The mechanical properties of three hybrid composites [G3C2]<sub>s</sub>, [G2C2G]<sub>s</sub>, and [GCG2C]<sub>s</sub> were investigated [8] in dry and seawater aged (90 days) conditions. The results data confirm that the hybrid composite absorbs less water than plain carbon and plain glass fiber polymer composite and all mechanical properties decrease with increasing aged time. The best mechanical properties is for the stacking sequence [GCG2C]<sub>s</sub> because of the presence of one glass ply at the exteriors where its flexural strength is 462 MPa in dry condition and decrease by 10.1% in aged condition. Two types of UD glass and carbon fiber were used [9] to form three hybrid composites (S-2 and T700S, S-2 and TR30S and E and TR30S) which is ordered in two stacking sequences of [0G/04C] and [02G/03C] and found that the compression failure is predominated. Therefore, putting glass fiber in the upper side and carbon fiber in the lower side of the laminated composites was better to get the best bending properties as long as glass volume fraction percentage does not exceed 25%. The catastrophic brittle fracture of CFRP composite can be minimized [10] by hybridization of 3k-carbon fabric with E-glass fabric alternatively in eight layers laminated composite via increasing the strain to failure (ductility) by 30% in comparison with CFRP composite during flexural test and increasing the flexural strength and modulus by 149% and 144% compared with GFRP composite. Alcludia-Zacarias et al. [11] demonstrated G:C hybrid ratio equal to 4:2, [GCG]<sub>s</sub> has the best tensile and bending mechanical properties, where the hybrid effects are ranged from 1.3 to 1.8. On the other hand, 2:4 G:C hybrid ratio [CGC]<sub>s</sub> has the best mechanical properties where the hybrid effects are ranged from 1.1 to 2.49. This is due to the presence of carbon between two layers of glass in the first case and vice versa in the second case.

### 1.2 Glass: Carbon: Kevlar Fiber Hybrid Composite

Song and Monjon et al. [12, 13] hybridize carbon fiber with glass and aramid fibers via coupling effects using the VARTM process. ACA and GCG have superior tensile strength and modulus compared to CAC and CGC. The tensile strength and stiffness of CG1 and CA1 are nearly identical because the carbon layer controls the mechanical properties of the laminate [12]. Bending strength and stiffness is higher than for carbon fiber followed by glass fiber, and finally, Kevlar fiber, and the opposite is right about the bending strain to failure, where the Kevlar fiber is more ductile followed by glass and finally, carbon fibers. 2G+6C has the highest bending strength and stiffness equal to 820 MPa and 38.8 GPa, respectively. For the pairing effect of glass/carbon in laminated composite by setting the glass on the compression side and carbon on the tension side. For the second group, 6G+2K has the highest bending strength and stiffness, which is equal to 696.5 MPa and 23.3 GPa, respectively, for the coupling effect of glass /Kevlar in laminated composite by setting glass in the compression side and Kevlar in the tension side. In the same manner, the coupling effect of carbon/Kevlar, 6C+2K has the highest bending strength and stiffness, which is equal to 645 MPa and 24.5 GPa, respectively, by setting the carbon fiber in the compression side and Kevlar in the tension side [13].

### 1.3 Interply and Intraply Hybrid Composite

Interply (inter-layer) and intraply (intra-layer) are two ways to hybridize low elongation fibers (carbon) with high-elongation fibers (glass). In the first one, the individual layer of fibers are stacked on each other in a different sequence, but in the second type, the combined fibers (yarn-to-yarn) are partnership in the same layer [14]. Researchers [2, 15, 16, 17, 18] investigated the mechanical properties for both inter-layer and intra-layer laminated composite. [2] studied the bending properties at different hybrid ratio G:C equal to 1:1, 2:1 and 4:1, and found that the hybrid ratio 1:1 gave the highest bending strength and modulus while the hybrid ratio 4:1 gave the highest strain to failure to the laminated composite. Ikbal et al. [15] used only the hybrid ratio G:C equal to 1:1 and found that the tensile and compression properties for intra-layer are higher a little bit than inter-layer. The flexural, tensile and compression properties were researched at various hybrid ratio G:C is equal to 1:1, 2:1, 3:1, 4:1, and various stacking sequences for the same hybrid ratio [16, 17]. It can get superior flexural properties by controlling the hybrid ratio and stacking sequence of glass and carbon for both inter-layer and intra-layer [16]. With increasing glass fiber content, the flexural modulus decreases and the strain to failure increases, while the flexural strength depends mainly on the stacking sequence. Increasing carbon content increased the tensile modulus and strength while the strain to failure decreased [17]. The tensile and compressive modulus for inter-layer and intra-layer are near each other for the same hybrid ratio and stacking sequence. The ratio of tensile strength to compression strength ( $R_{TC}$ ) mainly depends on the stacking sequence. When the glass fiber is at the outer surfaces,  $R_{TC}$  is minimized, and vice versa when the carbon fiber is at the outer surfaces of the laminated composite. Guo et al. [18] evaluated the interlaminar shear ISS, bending, and tensile strength for uniformly distributed intra-layer G/C hybrid rod composite, which are higher by 10.9%, 60.3%, 58.69% than interlayer (core-shell) glass/carbon hybrid rod composite.

### 1.4 Impact of Stacking Sequence and Angle of Orientation on Hybrid Composite

Agarwal et al. and Pujar et al. [19, 20] show the effect of stacking sequence and angle of orientation of glass and carbon on the mechanical properties of hybrid composites. They [19] used seven layers of glass/carbon and found that the best tensile strength was for stacking sequence GCGCGCG with 32% glass fabric and 18% carbon fabric content, while the best flexural strength was for stacking sequence CCGGGCC with 22% glass fabric and 28% carbon fabric content. Pujar et al. [20] demonstrated the mechanical properties of 10 layers of glass/carbon and found that the best tensile strength with arrangement [G4C]<sub>s</sub> at 0° angle of orientation increased by 37.5% compared with pure glass arrangement. The maximum bending strength for fiber arrangement [CG4]<sub>s</sub> was at 0° angle of orientation, which is increased by 10.5% compared with pure glass arrangement. Abd Ghani and Mahmud [21] used two stacking sequences

for both balanced hybrid G/C cross-ply and balanced hybrid G/C quasi-isotropic laminated composites. They concluded that the tensile modulus and strength for the balanced cross-ply [2G<sub>90°</sub>/2C<sub>0°</sub>/2G<sub>90°</sub>] were equal to 58.2724 GPa and 663.73 MPa, respectively and were higher than the balanced quasi-isotropic composite. The maximum flexural modulus and strength were evaluated for quasi-isotropic arrangement [2G<sub>0°</sub>/2G<sub>90°</sub>/2C<sub>±45°</sub>] which equal to 22.675 GPa and 797.77MPa, respectively.

**1.5 Nano Composite**

A perfect adhesion between matrix and fiber is required in order to modify the load transfer from the matrix to the fiber, in which nano or micro fillers powder is added to the matrix to enhance the load-carrying capacity of the hybrid laminated epoxy composite. The addition of nanofiller to the composite is in the range of 0-2% in order to avoid agglomeration of it in the matrix, which leads to a drop in mechanical properties [22]. The best method for mixing the nanofiller with epoxy resin is using a sonication mixer with a magnetic mixer at the same time by dual mixing process [23,24]. Adding nano alumina (Al<sub>2</sub>O<sub>3</sub>) concentration at weight percentages of 1, 2, 3, 4, and 5% to the epoxy matrix is to tough short carbon/glass fibers of length 1-7 mm. The optimum dispersion of nano Al<sub>2</sub>O<sub>3</sub> equals to 2 wt.% and improves the impact and flexural properties compared to neat epoxy [25]. Afrouzian et al. [26] investigated the tensile, bending and indentation quasi-static properties and ballistic impact dynamic properties for woven glass (12 layers) laminated epoxy composite toughened by several weight percentages of nano silica particles (0, 0.5, 1, and 3) and reached that the best nano SiO<sub>2</sub> that supply balanced mechanical properties is at a concentration of 0.5%. The less damaged area was found at 0.5% lower than the neat epoxy by 47% and 32% for quasi-static indentation and ballistic impact, respectively. In [27], carbon fiber laminated reinforced epoxy composite was toughened by different weight percentages of nano Al<sub>2</sub>O<sub>3</sub> at 1-5%, and found practically that the concentration of 2% nano Al<sub>2</sub>O<sub>3</sub> showed the highest tensile strength and strain, equal to 759.4 MPa and 3.73%, respectively, and the highest bending strength and strain, which were equal to 440.6 MPa and 1.32%, respectively. In addition to tension and bending, low-impact tests with velocities range of 2, 2.5, and 3 m/s were performed and found that the addition of 2% of nano Al<sub>2</sub>O<sub>3</sub> gave the highest impact force and less damage area. In [28], it is suggested that carbon/glass hybrid laminated epoxy composite toughened by 1.5% nano alumina and 1.5% nanographene to enhance the mechanical properties of wind turbine blades and characterized best dispersion of both nano in epoxy matrix through SEM for the fractured region in which fiber breakage with fiber pull-out cavity was recognized.

Based on the results of previous papers [4, 2, 15], which state that the best mechanical properties (tensile and flexural) can be achieved at a hybrid ratio of G:C equal to 1:1; therefore, in this work, two groups of laminated epoxy composites were fabricated by vacuum assisted resin infusion method, cross-laminate group and quasi laminate group, in which both of them containing equal numbers of carbon and glass fiber layers. Tensile and flexural behavior for each group with and without nano alumina were investigated and compared with each other. Finally, scanning electronic microscopy for four selected laminates which are Q2 and Q2WN tensile samples and C1 and C1WN bending samples, were photographed.

**2.0 EXPERIMENTAL WORK**

**2.1 Materials**

Laminating epoxy resin MGS L285 and its hardener 285 with a mixing ratio of 100:40 (resin: hardener) was used as a matrix. Unidirectional carbon fabric weight 300 g/cm<sup>2</sup> and its tow equal to 12K, and Unidirectional E-glass fabric weight 330 g/cm<sup>2</sup>, UD 0 -90- stitch, 0° = 283 gr, 90° = 37 gr, stitch fiber=10 gr were used as a fiber reinforcement. Both matrix and fiber were supplied from DOST KIMYA Company-Istanbul/Turkey. Spherical aluminum oxide (Al<sub>2</sub>O<sub>3</sub>) nanopowder/nanoparticle, 85% alpha, 15% gamma with 48 nm size, was used as a filler reinforcement and was supplied from Nanografi Nanotechnology Company, Ankara. The technical properties are shown in Table 1.

Table 1. L285 resin and H285 hardener properties

Properties	L285 resin	H285 hardener
Density (g/cm <sup>3</sup> )	1.18-1.23	0.94-0.97
Viscosity (mPa.s)	600-900	50-100
Epoxy equivalent, (g/equivalent)	155-170	-----
Amine value, (mg KOH/g)	-----	480-550
Refractory index	1.525-1.530	1.5020-1.5500

**2.2 Ultrasonic Dual Mixing Method**

Nano alumina powder (Al<sub>2</sub>O<sub>3</sub>) with a weight fraction of 2% was added to 370 g MGS L 285 epoxy base resin and premixed manually. The suspension (Al<sub>2</sub>O<sub>3</sub> +resin) was subjected to an ultrasonic dual mixing method (UDMM). Ultrasonic pulsed vibration stirrer with an amplitude of 70% and pulsed time equal to 2 sec on and 3 sec off (VCX 500, Sonics, USA) simultaneously along with magnetic stirrer at 350 rpm and 22 °C (MR Hei-Tech, Heidolph, Germany) were used for 2 hours in order to obtain uniformly distributed nano-particles in epoxy resin. So as to prevent too much temperature rise above 50 °C that leads to resin degradation during UDMM, an ice bath was provided around the suspension container, as shown in Figure 1(a). The vacuum degassing process came after UDMM for about 15 min to remove air bubbles (voids), which were initiated during mixing process as shown in Figure 1(b). Finally, the degassed

suspension was mixed with 148 g hardener and then drawn by vacuum to laminated fiber composite via vacuum-assisted resin infusion method.



Figure 1. Nano alumina and epoxy resin suspension mixing process, (a) UDMM, (b) vacuum chamber degassing process

### 2.3 Vacuum-assisted Resin Infusion Molding Process

Hybrid G/C laminated nanocomposite plates 50×50 cm were prepared by vacuum-assisted resin infusion molding process (VARIM), as shown in Figure 2. Each laminated composite consists of eight layers of fiber, four layers of carbon and four layers of glass. The weight fraction of fiber was 53%, where the ratio of glass to carbon by weight is 56.2:43.8. Table 2 shows the stacking sequence configuration for symmetrically laminated epoxy composite.

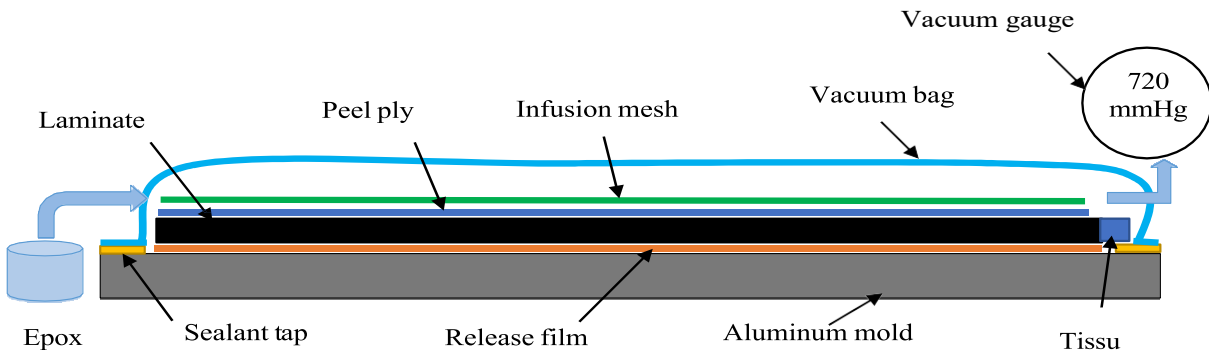


Figure 2. Laminated composite epoxy composite fabricated by VARIM

Table 2. Stacking sequence G:C configuration of hybrid laminated epoxy composites

Symbol	Laminates	Stacking sequence	Hybrid ratio G:C	Density (kg/m <sup>3</sup> )	Thickness (mm)
C1	Cross no.1	[G0/C90/C0/G90]s	4:4	1651.3	2.07
C1WN	Cross no.1 with nano Al <sub>2</sub> O <sub>3</sub>	[G0/C90/C0/G90]s	4:4	1686.0	2.07
C2	Cross no.2	[G0/G90/C0/C90]s	4:4	1653.5	1.90
C2WN	Cross no.2 with nano Al <sub>2</sub> O <sub>3</sub>	[G0/G90/C0/C90]s	4:4	16762	2.00
Q1	Quasi no.1	[G0/C90/C45/G-45]s	4:4	1679.6	1.91
Q1WN	Quasi no.1 with nano Al <sub>2</sub> O <sub>3</sub>	[G0/C90/C45/G-45]s	4:4	1681.0	1.95
Q2	Quasi no.2	[G0/G90/C45/C-45]s	4:4	1692.5	2.04
Q2WN	Quasi no. 2 with nano Al <sub>2</sub> O <sub>3</sub>	[G0/G90/C45/C-45]s	4:4	1702.7	2.05

All eight plies of dry fabric were cut off and positioned over release film that was fixed over an aluminum sandwich mold by using two edges sealant tape. After that, peel ply was placed over them, where on its side, there was a number of tissues set in between to absorb excessive epoxy. The next layer was infusion mesh which was used to force the toughened epoxy to distribute uniformly through the surface. Finally, the system is enclosed by using a vacuum bag. Before toughened epoxy was withdrawn, the temperature of the aluminum mold increased steeply to 30 °C in order to remove voids from the closed system. The vacuum was started with a pressure of 720 mmHg, and it should be constant. Otherwise, there would be a leakage in the system that must be solved. When the enclosed system with its connecting apparatus was satisfactory, the toughened epoxy was drawn by vacuum through an infusion hose to the laminated composite system, which was left at 80 °C for 15 hours to cure by using automatic control of VARIM [29]. The laminated composite plates of average thickness equal to 2 mm were cut according to the ASTM standard dimensions by using a water-jet cutting machine to prepare the tensile and flexural samples.

## 2.4 Mechanical Test

The mechanical behavior of the produced laminated composites was evaluated from five samples for each tensile and flexural test. The prepared tensile sample dimensions were 250×25×2 mm according to ASTM D3039 [30]. Four glass/epoxy tabs were added to the ends of the tension sample in order to prevent stress concentration at the fixture position. The prepared flexural sample dimensions were 100×12.7×2 mm according to ASTM D 790 [31]. The three-point flexural test was arranged by positioning the standard rectangular flexural sample between two roller supports of 30 mm diameter with a 60 mm span length, while the nose load point diameter was equal to 10 mm at the mid-point of the sample. The experimental flexural strength, strain, and modulus were evaluated according to the following equations [31].

$$\sigma_f = \frac{3 PL}{2 b d^2} \quad (1)$$

$$\varepsilon_f = \frac{6 D d}{L^2} \quad (2)$$

where  $\sigma_f$  is flexural strength in MPa,  $\varepsilon_f$  is flexural strain in mm/mm,  $P$  is load in N, and  $D$  is the central deflection of the beam in mm. The tensile and flexural tests were carried out using Shimadzu AGS-X Plus Universal Testing Machine (100 KN load Cell) with loading rates equal to 2 mm/min for the tension test and 1 mm/min for the flexural test, as shown in Figure 3.

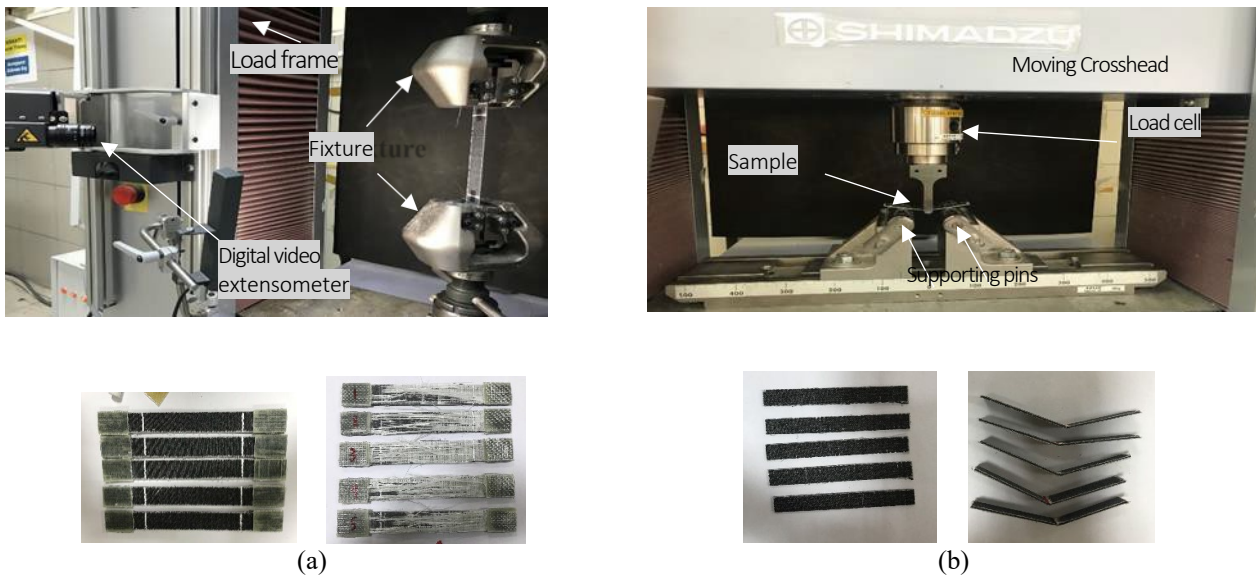


Figure 3. Samples and experimental test arrangement of (a) tensile test and (b) 3-point flexural test

## 3.0 RESULTS AND DISCUSSION

### 3.1 Tensile Test Results

Tensile stress-strain curves for the eight laminated glass/carbon epoxy (cross and quasi) composites are shown in Figure 4(a) and 4(b), respectively. All laminated epoxy composite behaved linearly in the elastic region until the ultimate point. Debonding between fibers and matrix occurred in both cross and quasi-laminated composites before burst load drop (delamination). Little debonding occurred in cross-compared with quasi-laminated composites, which were backed by the presence of two layers of 0° carbon fabric in the first one and two layers of carbon fabric with either 90° or ±45° in the other.

Therefore, ultimate tensile strength and stiffness, alongside with burst load drop of quasi-laminated composites, were lower than that of cross one because debonding decreases the slope of stress-strain curve and leads to more separation between fiber and matrix similar to the results of research [21]. Both Table 3 and Figure 5 demonstrate the tensile properties of all laminated epoxy composites. In order to increase load carrying capacity, Nano- Al<sub>2</sub>O<sub>3</sub> was added to both stacking sequence [G/C/C/G/G/C/C/G], [G/G/C/C/C/C/G/G] of cross (C1, C2) and quasi (Q1, Q2) laminates via increasing the adhesion between fibers and epoxy matrix; therefore, samples C1WN, C2WN, Q1WN, and Q2WN are more deformable with higher ultimate tensile strength, ultimate tensile strain and tensile modulus than C1, C2, Q1, and Q2 respectively as shown in Figure 6 and Table 3 similar to the results of previous researches [22, 27].

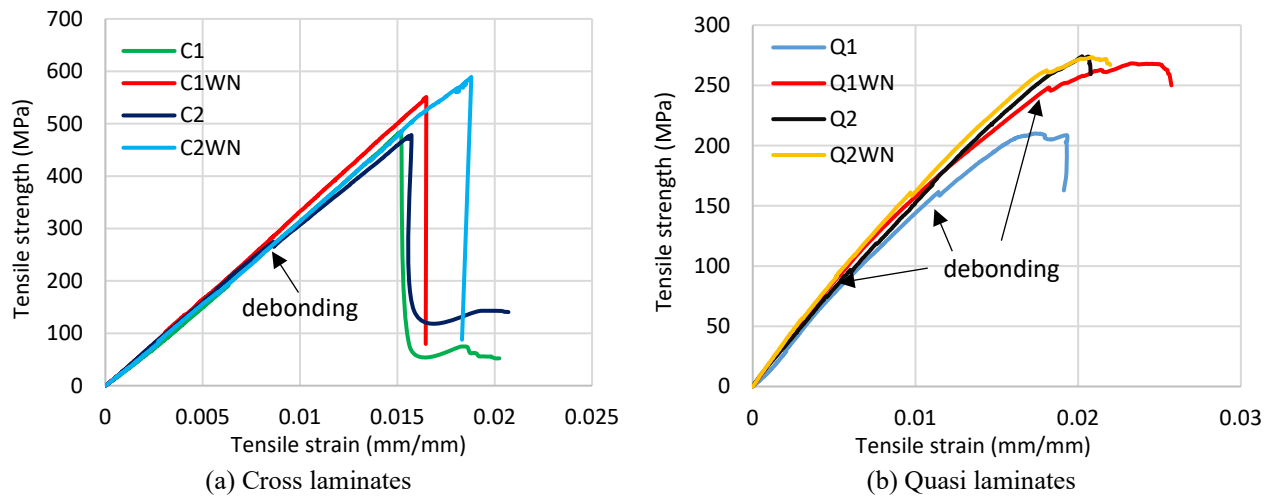


Figure 4. Tensile stress-strain curves for both symmetrical hybrid cross and quasi-laminated epoxy composite with and without nano- $\text{Al}_2\text{O}_3$

Table 3. Tensile properties of the laminated epoxy composites

Laminates symbol	Ultimate tensile strength (MPa)	Ultimate tensile strain (%)	Tensile modulus, $E_t$ (GPa)
C1	523	1.39	34.321
C1WN	593	1.53	37.756
C2	518	1.44	34.762
C2WN	628	1.74	36.189
Q1	231	1.65	13.896
Q1WN	285	1.88	15.721
Q2	292	1.9	15.012
Q2WN	294	1.98	16.409

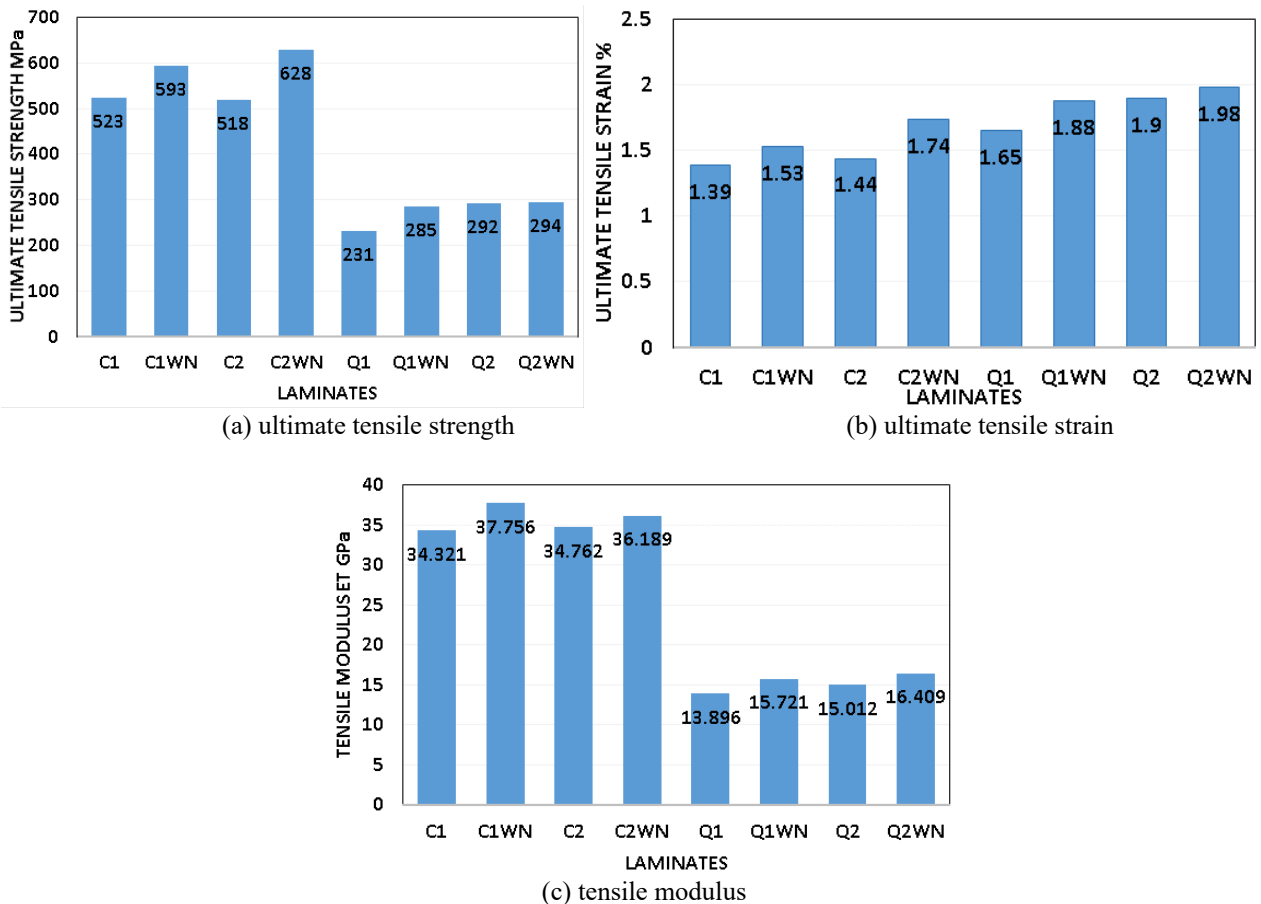


Figure 5. Tensile properties for both cross and quasi laminated epoxy composite with and without nano- $\text{Al}_2\text{O}_3$

It was obvious that C2WN has maximum tensile strength 628 MPa and a maximum tensile strain of 1.74% because of the presence of four carbon plies in the middle of the laminate, while C1WN has a maximum tensile modulus of 37.756

GPa, which is higher than the tensile modulus of C2WN by 4.2% in cross-laminate group, both of them are characterized by high glass fiber pull-out at the outer surface after carbon fiber underneath breakage represented as the white spot with internal delamination. Quasi laminated group is characterized by high off-axis shear stress at  $\pm 45^\circ$  which led to severe internal delamination with little glass fiber pull-out and little carbon fiber breakage, similar to the results of [21], as shown in Figure 6. Q2WN has the maximum tensile properties (strength, strain, and modulus), which are equal to 294 MPa, 1.98% and 16.409 GPa, respectively, in the quasi-group laminate because of the presence of four carbon layers in the middle of the laminate with  $\pm 45^\circ$  angle of orientation.



Figure 6. Tensile failure modes for both cross and quasi-laminated epoxy composite with and without Nano- $\text{Al}_2\text{O}_3$

Theoretical tensile modulus,  $E_t$ , was predicted by using classical laminate theory by using the data shown in Table 4, which represent the mechanical properties of unidirectional glass and carbon with and without nano-alumina, and then compared with the experimental one listed in Table 3 as shown in Figure 7. It was evident that the theoretical tensile modulus,  $E_t$ , is higher than that the experimental one, and that is due to the classical laminate theory assuming perfect bonding between fibers and matrix but in reality, it is not true. The extensional stiffness matrix and longitudinal tensile modulus for each laminate can be calculated by using the following equations [32]

$$A_{ij} = \sum_{k=1}^n [(\bar{Q}_{ij})]_k (h_k - h_{k-1}), \quad i, j = 1, 2, 6 \quad (3)$$

$$E_t = \frac{1}{h A_{11}^*} \quad (4)$$

where  $A_{ij}$  = extensional stiffness matrix (Pa.m),  $\bar{Q}_{ij}$  = reduced stiffness matrix (Pa),  $h$  = laminate thickness (mm),  $A_{11}^*$  = first element in extensional compliance matrix ( $\frac{1}{\text{Pa.m}}$ ), and  $E_t$  = longitudinal tensile modulus (GPa).

Table 4. The mechanical properties of unidirectional glass and carbon with and without nano- $\text{Al}_2\text{O}_3$

Laminates	Density (kg/m <sup>3</sup> )	$E_1$ (MPa)	$E_2$ (MPa)	$\nu_{12}$	$G_{12}$ (MPa)
UD glass/epoxy	1658	31802	12804	0.22	4271
UD carbon/epoxy	1484	99438	6273	0.25	4031
UD glass/epoxy $\text{Al}_2\text{O}_3$	1883	33507	13344	0.27	4500
UD carbon/epoxy $\text{Al}_2\text{O}_3$	1574	105044	6626	0.30	4260

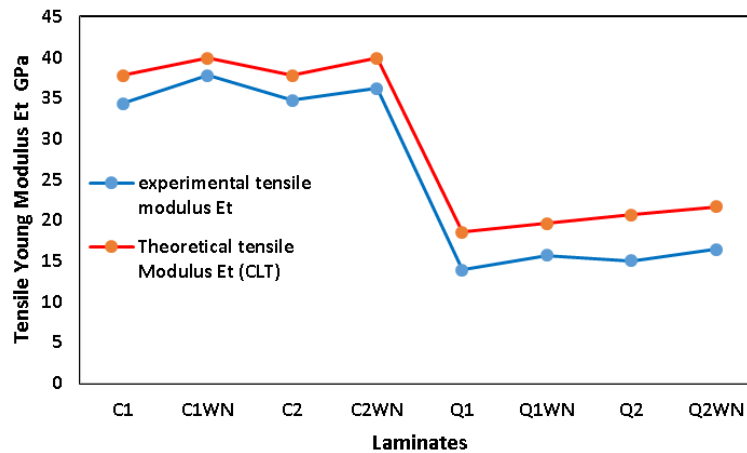


Figure 7. Experimental and theoretical tensile modulus  $E_t$  difference

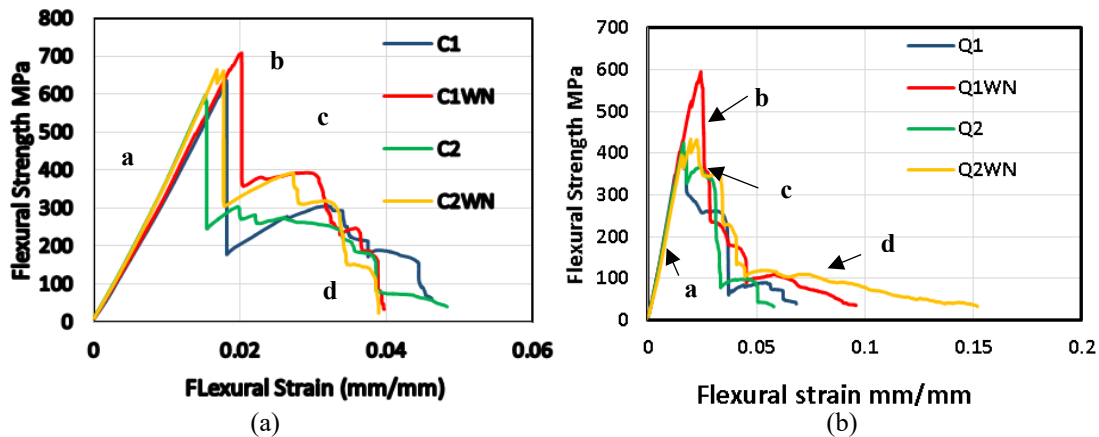
Table 5 demonstrates the  $[A]$  matrix and theoretical tensile modulus,  $E_t$ , for each laminated epoxy composite. It was clear that the extensional matrix  $[A]$  and  $E_t$  theoretical is higher for C1WN and C2WN because of the presence of two  $0^\circ$  carbon layer fiber in the laminate, which was given the ability to resist more elongated load. Although stacking sequence of C1WN and C2WN was different, the theoretical  $E_t$  is the same because both had two  $0^\circ$ ,  $90^\circ$  carbon fiber and two  $0^\circ$ ,  $90^\circ$  glass fiber. The same thing does not apply to the quasi-group because of the different angles of orientation of the fibers for the different stacking sequences. Q2WN had the maximum theoretical tensile modulus 21.7 GPa in the quasi-group.

### 3.2 Flexural Test Results

Flexural stress-strain curves for the eight laminated glass/carbon epoxy (cross and quasi) composites were passed through four stages (a) elastic stage, (b) compressive failure stage, (c) hill failure stage (plateau), and (d) tensile failure stage are shown in Figure 8(a), and 8(b), respectively similar to the results of researches in [11, 21]. All laminated epoxy composites behaved linearly in the elastic region until the ultimate point, along with the occurrence of a small amount of debonding in the quasi-group. Laminates were subjected to flexural load in the compressive region, which then shifted through it to the tensile region; since the laminates were symmetric then, the compressive and tensile stresses were equivalent to each other. As the compressive layers failed, the load-carrying capacity transferred to the tension layers through stage c was characterized by load rising before tensile layer failure, similar to research [11]. The plateau stage for the quasi-laminate group is little or absent, but the tension failure stage is longer than the cross-laminate group. In general, the flexural failure modes are characterized by fiber buckling at the compression side and fiber breakage or fiber pull-out on the tension side with little internal delamination and transverse crack propagation, as shown in Figure 10 similar to the results of previous researches [9, 11, 21].

Table 5. Extensional stiffness matrix [A] and theoretical tensile modulus, Et

Laminates	Extensional matrix [A]*10 <sup>6</sup> (Pa.m)	Theoretical E <sub>t</sub> (GPa)
C1	$\begin{bmatrix} 75.8 & 4.4 & 0 \\ 4.4 & 75.8 & 0 \\ 0 & 0 & 8.3 \end{bmatrix}$	37.8
C1WN	$\begin{bmatrix} 80.28 & 5.71 & 0 \\ 5.71 & 80.28 & 0 \\ 0 & 0 & 8.76 \end{bmatrix}$	39.9
C2	$\begin{bmatrix} 75.8 & 4.4 & 0 \\ 4.4 & 75.8 & 0 \\ 0 & 0 & 8.3 \end{bmatrix}$	37.8
C2WN	$\begin{bmatrix} 80.28 & 5.71 & 0 \\ 5.71 & 80.28 & 0 \\ 0 & 0 & 8.76 \end{bmatrix}$	39.9
Q1	$\begin{bmatrix} 43.6 & 18.14 & 9.27 \\ 18.14 & 80.7 & 9.27 \\ 9.27 & 9.27 & 2.2 \end{bmatrix}$	18.52
Q1WN	$\begin{bmatrix} 46.46 & 19.97 & 9.78 \\ 19.97 & 46.46 & 9.78 \\ 9.78 & 9.78 & 23.02 \end{bmatrix}$	19.62
Q2	$\begin{bmatrix} 54.1 & 26.2 & 0 \\ 26.2 & 54.1 & 0 \\ 0 & 0 & 30.02 \end{bmatrix}$	20.7
Q2WN	$\begin{bmatrix} 57.46 & 28.53 & 0 \\ 28.53 & 57.46 & 0 \\ 0 & 0 & 31.58 \end{bmatrix}$	21.7


 Figure 8. Flexural stress-strain curves for symmetrical hybrid laminated epoxy composite with and without nano-Al<sub>2</sub>O<sub>3</sub>: (a) cross laminates, (b) quasi laminates

Both Table 6 and Figure 9 demonstrate flexural properties of all laminated epoxy composites. In order to increase load carrying capacity, nano- Al<sub>2</sub>O<sub>3</sub> was added to both stacking sequence [G/C/C/G/G/C/C/G], [G/G/C/C/C/C/G/G] of cross (C1, C2) and quasi (Q1, Q2) laminates via increasing the adhesion between fibers and epoxy matrix; therefore, samples C1WN, C2WN, Q1WN, and Q2WN are more deformable with higher ultimate flexural strength, ultimate flexural strain and flexural modulus than C1, C2, Q1, and Q2 respectively as shown in Figure 10 and Table 6 similar to the results of researches [22, 25, 27] It was obvious that the stacking sequence G/C/C/G/G/C/C/G with Nano-Al<sub>2</sub>O<sub>3</sub> for both cross and quasi groups have the best flexural properties than G/G/C/C/C/C/G/G because of the presence of carbon layer near the outer surfaces of the laminates far from the neutral axis. Generally, the cross-laminate C1WN has two 0° carbon fiber layers, so the flexural properties were the best among the other laminates. C1WN had the maximum flexural strength 708.2 MPa and maximum flexural strain 2.027%, while C2WN had the maximum flexural modulus of 38.73 GPa in the cross-laminate group. In the quasi group, Q1WN had the maximum flexural properties (strength, strain, and modulus) which are equal to 596 MPa, 2.424% and 29.2 GPa, respectively.

Table 6. Flexural properties of the laminated epoxy composites

Laminates symbol	Ultimate flexural strength (MPa)	Ultimate flexural strain (%)	Flexural modulus, $E_b$ (GPa)
C1	635.3	1.82	34.01
C1WN	708.2	2.027	35
C2	598	1.533	38.14
C2WN	664.4	1.689	38.73
Q1	401	1.625	26.63
Q1WN	596	2.424	29.2
Q2	425	1.628	26.26
Q2WN	434.2	1.955	27.01

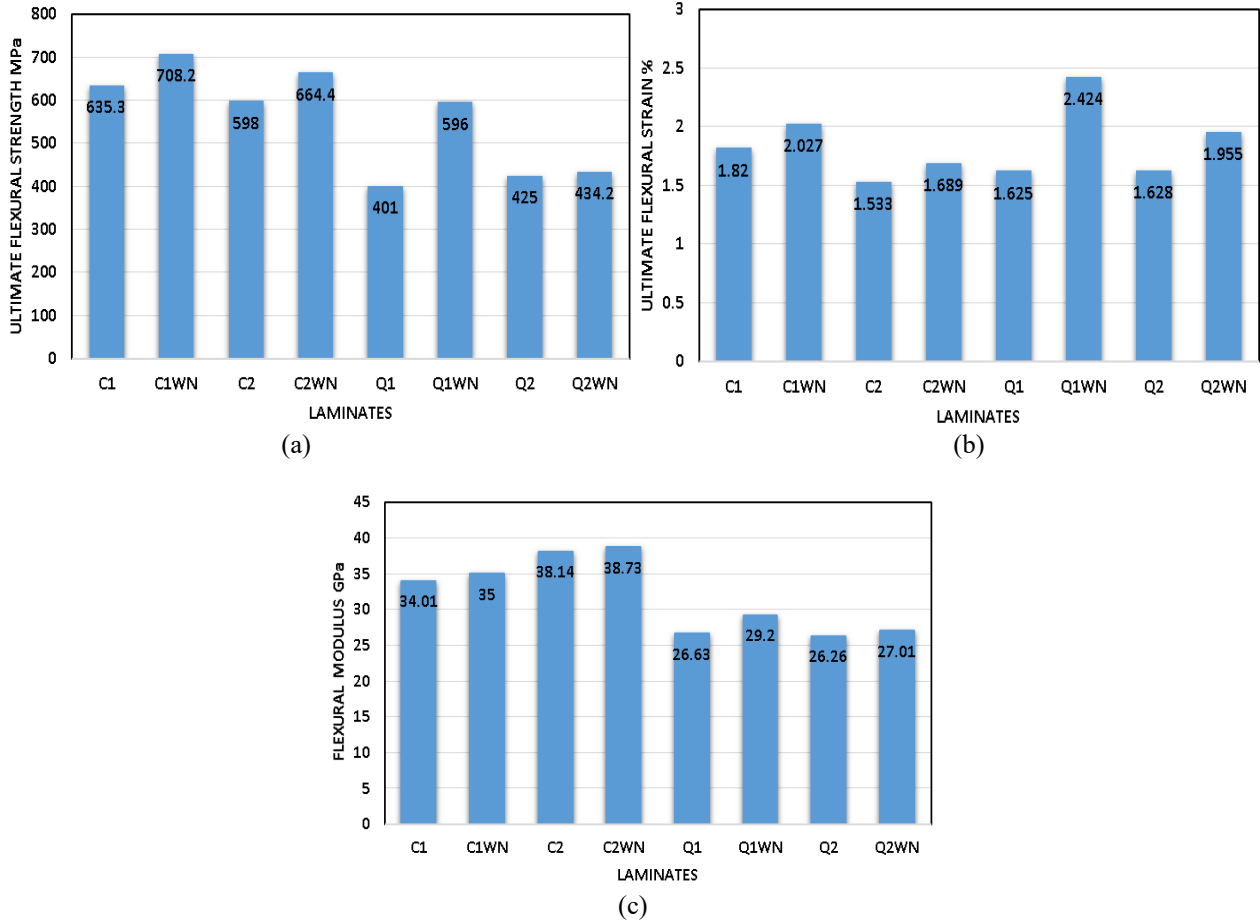
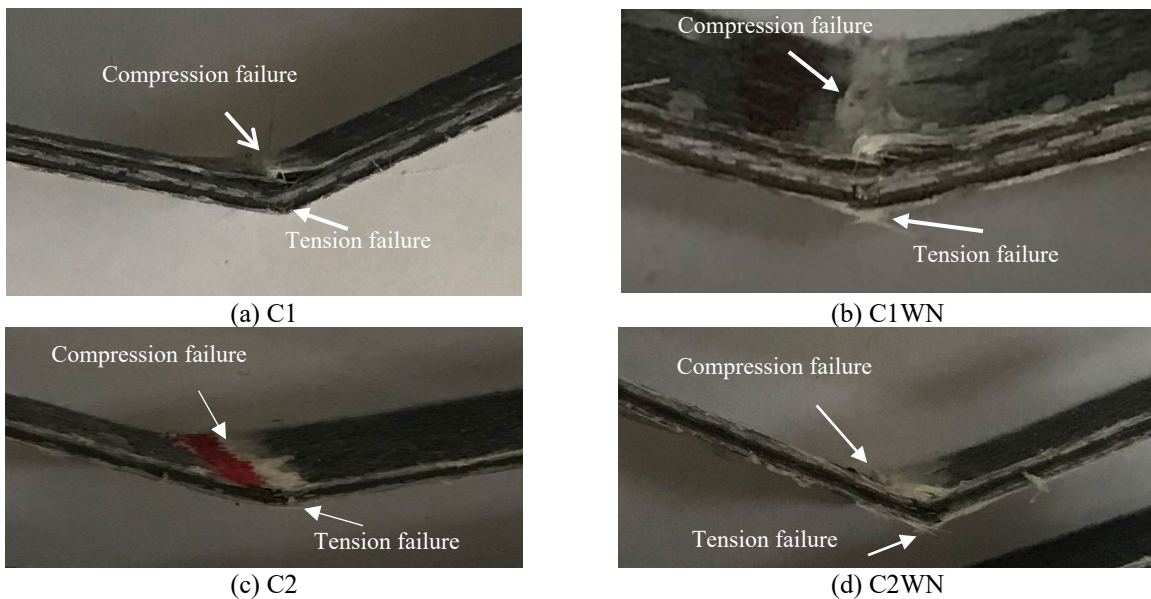


Figure 9. Flexural properties for both cross and quasi-laminated epoxy composite with and without nano- $Al_2O_3$ : (a) ultimate flexural strength, (b) ultimate flexural strain



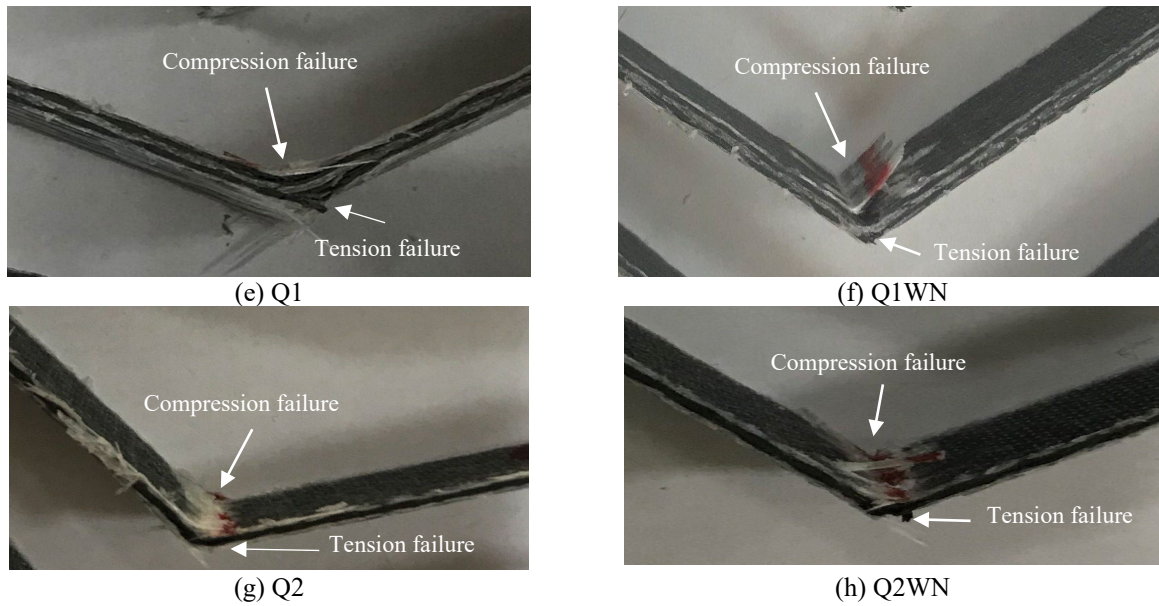


Figure 10. Flexural failure modes for both cross and quasi-laminated epoxy composite with and without nano- $\text{Al}_2\text{O}_3$

Theoretical flexural modulus,  $E_b$ , was predicted by using classical laminate theory by using the data shown in Table 4, which represent the mechanical properties of unidirectional glass and carbon with and without nano-alumina, and then they compared with the experimental one listed in Table 6 as shown in Figure 11. It was evident that the theoretical flexural modulus,  $E_b$ , is lower than that of the experimental one, returns that classical laminate theory neglect the effect of transverse shear (shear due to bending) presence between layers. The flexural stiffness matrix and flexural modulus for each laminate can be calculated by using the following equation [32].

$$D_{ij} = \frac{1}{3} \sum_{k=1}^n [(\bar{Q}_{ij})]_k (h_k^3 - h_{k-1}^3), \quad i, j = 1, 2, 6 \quad (5)$$

$$E_b = \frac{12}{h^3 D_{11}^*} \quad (6)$$

where  $D_{ij}$  = flexural stiffness matrix ( $\text{Pa}\cdot\text{m}^3$ ),  $\bar{Q}_{ij}$  = reduced stiffness matrix (Pa),  $h$  = laminate thickness (mm),  $D_{11}^*$  = first element in flexural compliance matrix ( $\frac{1}{\text{Pa}\cdot\text{m}^3}$ ), and  $E_b$  = longitudinal flexural modulus (GPa).

Table 7 demonstrate the flexural stiffness [D] matrix and theoretical flexural modulus,  $E_b$ , for all laminated epoxy composites. It was obvious that C2WN had the maximum theoretical flexural modulus 35.1 GPa, which returns to its maximum flexural stiffness matrix [D] in the cross group. Q2WN had the maximum theoretical flexural modulus 26 GPa in the quasi group, which returns to its maximum flexural stiffness matrix [D] in the same group, but experimentally Q1WN had the maximum modulus.

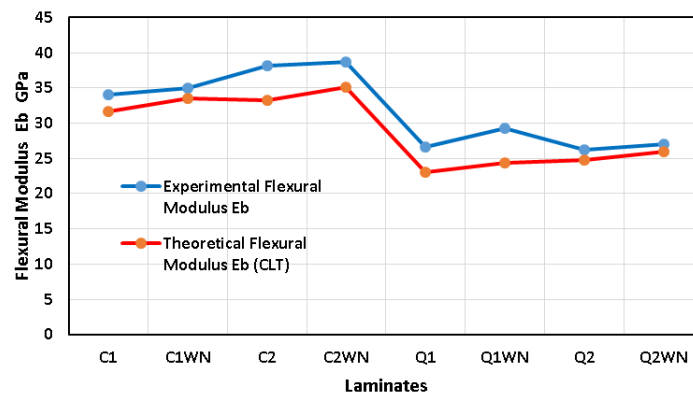


Figure 11. Experimental and theoretical flexural modulus,  $E_b$ , difference

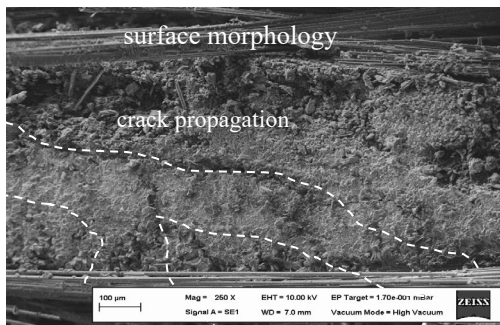
### 3.3 Morphology from Scanning Electron Microscopy

The scanning electronic microscopy SEM was to oversight and observe the morphology of the internal structure of the laminates through the adhesion between fibers and matrix and noticing the failure modes, which its affect totally on the mechanical properties of the laminated epoxy composites [10]. Specimens of dimensions  $10 \times 10$  mm were cut from the flat fractured area of Q2, Q2WN tensile samples and C1, C1WN flexural samples and their sides were polished via

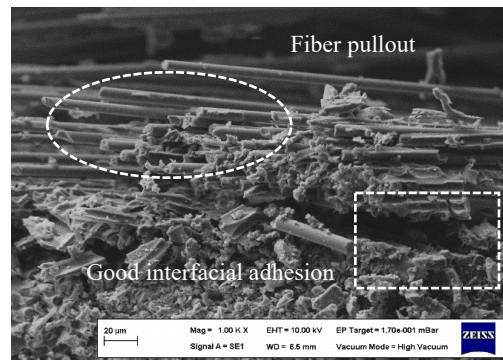
sand papers to achieve flat smooth sides, which are then coated by gold and then scanned by using Zeiss EVo 50 scanning electron microscope operating at 25 KV. Q2 and Q2WN tensile samples and C1 and C1WN flexural samples were scanned as shown in Figures 12, 13, 14, and 15 respectively.

Table 7. Flexural matrix [D] and theoretical flexural modulus,  $E_b$

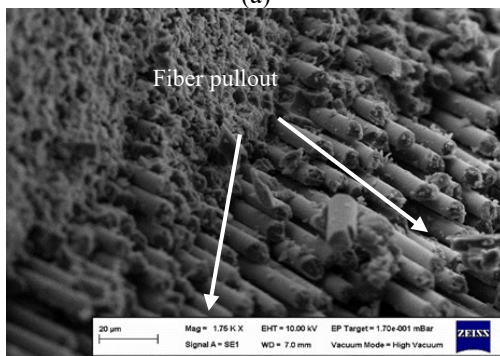
Laminates	Flexural matrix [D] (Pa.m <sup>3</sup> )	Theoretical $E_b$ (GPa)
C1	$\begin{bmatrix} 21.2 & 1.56 & 0 \\ 1.56 & 25.6 & 0 \\ 0 & 0 & 2.78 \end{bmatrix}$	31.6
C1WN	$\begin{bmatrix} 22.46 & 2.01 & 0 \\ 2.01 & 27.05 & 0 \\ 0 & 0 & 2.94 \end{bmatrix}$	33.5
C2	$\begin{bmatrix} 22.43 & 1.81 & 0 \\ 1.81 & 12.95 & 0 \\ 0 & 0 & 2.83 \end{bmatrix}$	33.3
C2WN	$\begin{bmatrix} 23.79 & 2.33 & 0 \\ 2.33 & 13.71 & 0 \\ 0 & 0 & 2.98 \end{bmatrix}$	35.1
Q1	$\begin{bmatrix} 16.21 & 3.21 & 1.65 \\ 3.21 & 27.26 & 1.65 \\ 1.65 & 1.65 & 4.43 \end{bmatrix}$	23
Q1WN	$\begin{bmatrix} 17.24 & 3.74 & 1.75 \\ 3.74 & 28.83 & 1.75 \\ 1.75 & 1.75 & 4.66 \end{bmatrix}$	24.4
Q2	$\begin{bmatrix} 17.7 & 3.62 & 1.46 \\ 3.62 & 14.07 & 1.46 \\ 1.46 & 1.46 & 4.64 \end{bmatrix}$	24.75
Q2WN	$\begin{bmatrix} 18.8 & 4.23 & 1.55 \\ 4.23 & 14.91 & 1.55 \\ 1.55 & 1.55 & 4.88 \end{bmatrix}$	26



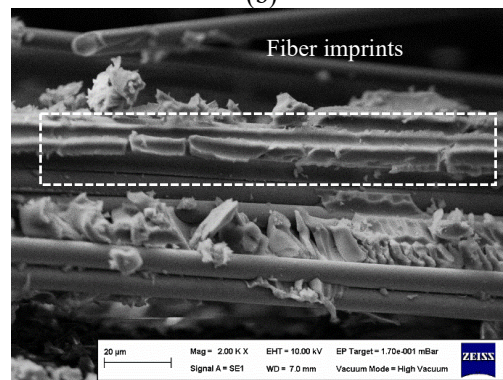
(a)



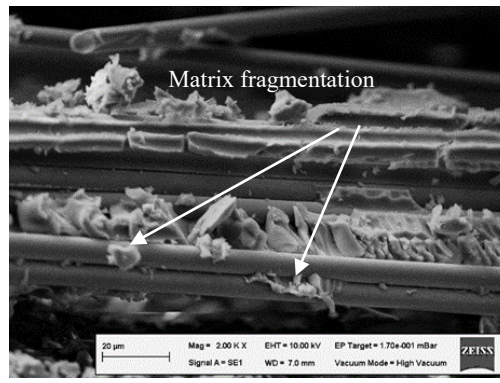
(b)



(c)

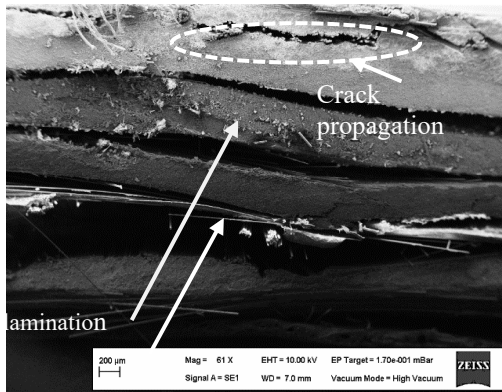


(d)

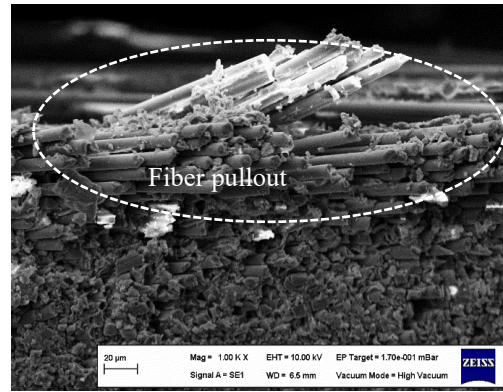


(e)

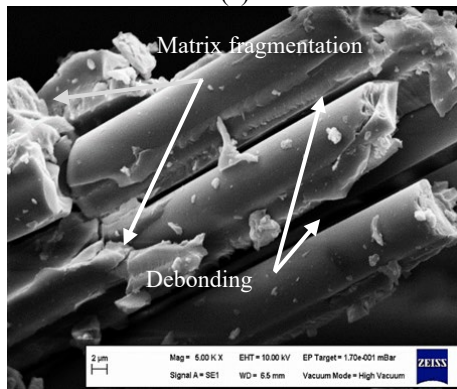
Figure 12. SEM of Q2 quasi laminate tensile sample: (a) crack propagation, (b) good interfacial adhesion, (c) fiber pull-out, (d) fiber imprints, (e) matrix fragmentation



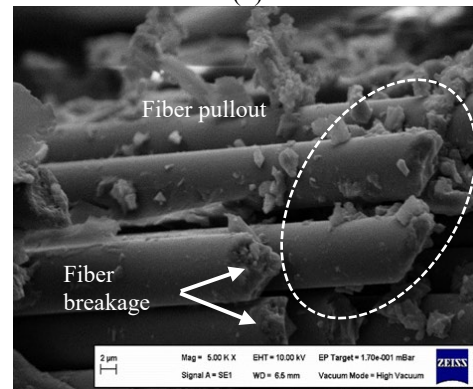
(a)



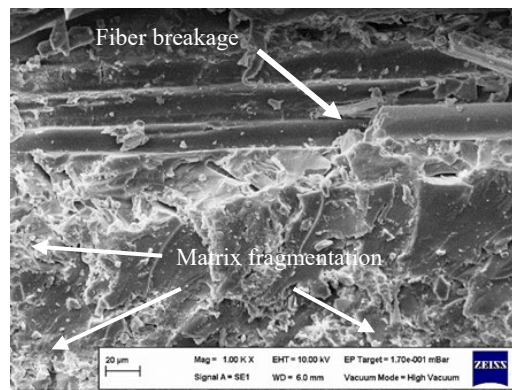
(b)



(c)



(d)



(e)

Figure 13. SEM of Q2WN quasi laminate tensile sample: (a) crack propagation, (b) Fiber pull-out, (c) debonding, (d) fiber breakage, (e) matrix fragmentation

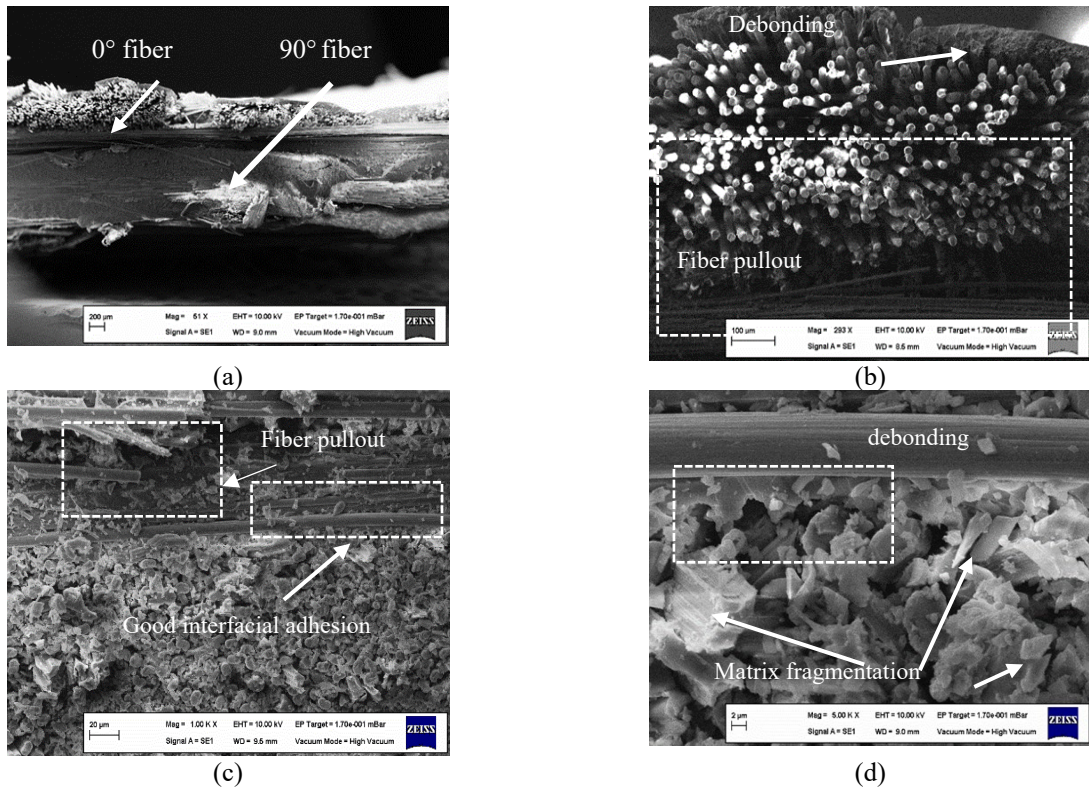


Figure 14. SEM of C1 cross laminate flexural sample: (a) 0° fiber and 90° fiber at failed region, (b) fiber pull-out, (c) good interfacial adhesion, (d) matrix fragmentation

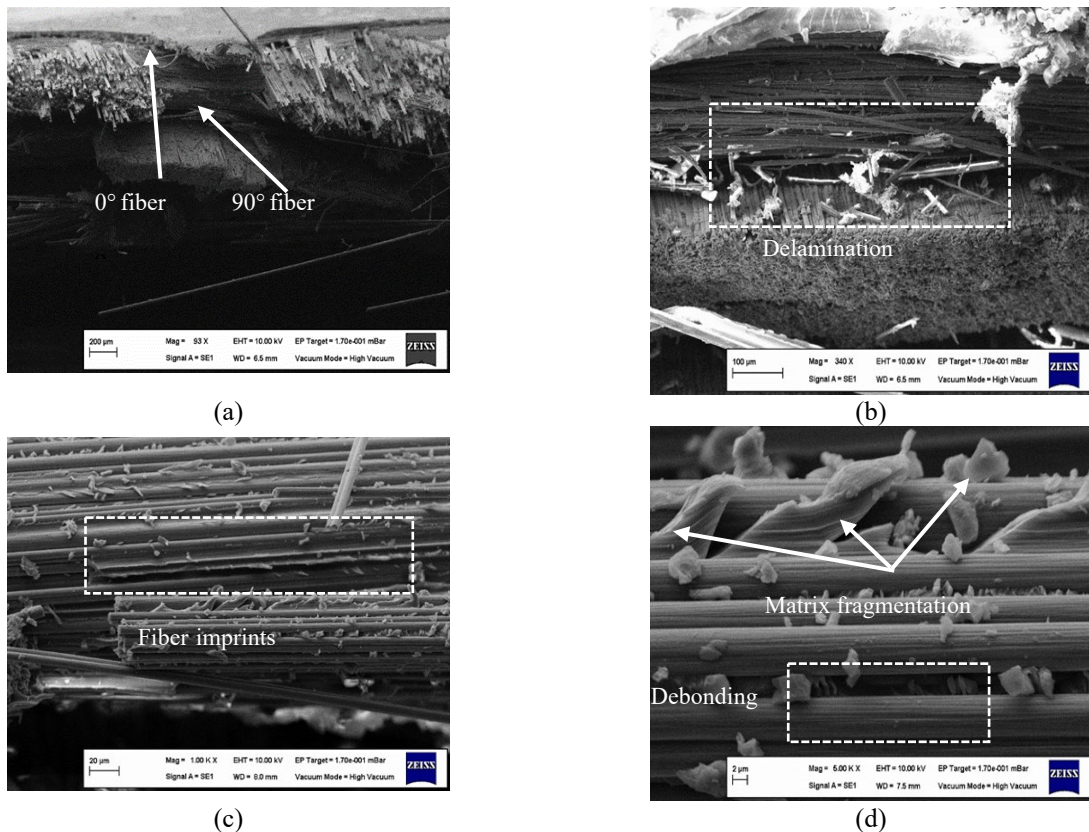


Figure 15. SEM of C1WN cross laminate flexural sample: (a) 0° fiber and 90° fiber at the failed region, (b) delamination (c) fiber imprints, and (d) matrix fragmentation

The SEM morphology gave us a clear picture about the types of failure in both tensile and flexural samples like transverse matrix crack propagation, delamination, fiber pull-out and fiber breakage, matrix fragmentation and fiber imprints. Delamination may either occur between glass and carbon layers or between carbon and carbon layers. It was obvious from SEM that Q2, Q2WN, C1 and C1WN were failed by fiber pull-out and breakage more than that by debonding between them.

## 4.0 CONCLUSIONS

In this paper, two groups of laminates were fabricated; cross-laminate and quasi-laminate. The mechanical behavior of the two groups under two different stacking sequences with and without nano- $\text{Al}_2\text{O}_3$  was investigated by using quasi-static tensile and flexural tests. Adding 2% Nano  $\text{Al}_2\text{O}_3$  increases the mechanical tensile and flexural properties of all laminates (strength, strain and modulus). In the cross-laminate group, C2WN had the maximum tensile strength of 628 MPa and maximum tensile strain of 1.74%, while C1WN had the maximum tensile modulus of 37.756 GPa, which is higher than the tensile modulus of C2WN 36.189 GPa by 4.2%, but theoretically, both C1WN and C2WN have the same tensile modulus of 39.9 GPa, because both laminates have the same number of glass and carbon fiber with the same angle of orientation. The extensional stiffness matrix [A] does not depend on the position of the fiber layer in the overall laminate. In the quasi group, Q2WN had the maximum tensile properties (strength, strain, and modulus). On the other hand, the flexural properties for cross and quasi groups were evaluated. C1WN has a maximum flexural strength of 708.2 MPa and a maximum flexural strain of 2.027%, while C2WN had the maximum flexural modulus of 38.73 GPa in the cross group. In the quasi group, Q1WN has a maximum flexural strength of 596 MPa, maximum flexural strain of 2.424 % and maximum flexural modulus of 29.2 GPa, in spite of the fact that Q2WN has a maximum theoretical flexural modulus of 26 GPa in the quasi group. In general, the theoretical tensile modulus for all laminates was higher than the experimental one and vice versa for the flexural modulus. It was cleared from SEM that the laminates failed by fiber pull-out and fiber breakage rather than debonding, which is an indication of good adhesion between fibers and epoxy matrix.

For future work, it is suggested to exchange the glass fiber layer by carbon and the carbon fiber layer by glass for the same hybrid ratio of 4:4 and re-evaluation of mechanical behavior for all laminates, and finally compare with this paper.

## 5.0 ACKNOWLEDGEMENT

Thanks and appreciation to the head and staff of technical Mechanical and Energy Engineering Department, Erbil Technical Engineering College, Erbil Polytechnic University, Erbil, Iraq for providing all facilities to complete this work.

## 6.0 REFERENCES

- [1] I.M. Daniel, *Engineering Mechanics of Composite Materials*, United State of America: Oxford University Press, 2006.
- [2] M.H. Ikbali, Q.T. Wang, and W. Li, "Effect of glass/carbon ratios and laminate geometry on flexural properties of glass/carbon fiber hybrid composites," In: International Conference on Materials Chemistry and Environmental Protection 2015, Atlantis Press, p. 114–118, 2016.
- [3] G.A. Kretsis, "A review of the tensile, compressive, flexural and shear properties of hybrid fibre-reinforced plastics," *Composites*, vol. 18, no. 1, pp. 13–23, 1987.
- [4] J. Zhang, K. Chaisombat, S. He, and C.H. Wang, "Hybrid composite laminates reinforced with glass/carbon woven fabrics for lightweight load bearing structures," *Materials and Design*, vol. 36, pp. 75–80, 2012.
- [5] D.K. Jesthi, A. Nayak, S.S. Mohanty, A.K. Rout, and R.K. Nayak, "Evaluation of mechanical properties of hybrid composite laminates reinforced with glass/carbon woven fabrics," *IOP Conference Series: Materials Science and Engineering*, IOP Publishing, p. 12157, 2018.
- [6] D.K. Jesthi, S.S. Mohanty, A. Nayak, A. Panigrahi, and R.K. Nayak, "Improvement of mechanical properties of carbon/glass fiber reinforced polymer composites through inter-ply arrangement," *IOP Conference Series: Materials Science and Engineering*, IOP Publishing, p. 12182, 2018.
- [7] D.K. Jesthi, P. Mandal, A.K. Rout, and R.K. Nayak, "Effect of carbon/glass fiber symmetric inter-ply sequence on mechanical properties of polymer matrix composites," *Procedia Manufacturing*, vol. 20, pp. 530–5, 2018.
- [8] D.K. Jesthi, and R.K. Nayak, "Improvement of mechanical properties of hybrid composites through interply rearrangement of glass and carbon woven fabrics for marine application," *Composites Part B: Engineering*, vol. 168, pp. 467–75, 2019.
- [9] C. Dong, and I.J. Davies, "Flexural properties of glass and carbon fiber reinforced epoxy hybrid composites," *Proceedings of the Institution of Mechanical Engineers, Part L: Journal of Materials: Design and Applications*, vol. 227, no. 4, pp. 308–17, 2013.
- [10] T. Khan, A. Fikri, M.S. Irfan, E. Gunister, and R. Umer, "The effect of hybridization on microstructure and thermo-mechanical properties of composites reinforced with different weaves of glass and carbon fabrics," *Journal of Composite Materials*, vol. 55, no. 12, pp. 1635–51, 2021.
- [11] E. Alcudia-Zacarias, A. Abúndez-Pliego, J. Mayén, J. Colín-Ocampo, A. Blanco-Ortega, and W.M. Alcocer-Rosado, "Experimental assessment of residual integrity and balanced mechanical properties of GFRP/CFRP hybrid laminates under tensile and flexural conditions," *Applied Composite Materials*, vol. 27, no. 6, pp. 895–914, 2020.
- [12] J.H. Song, "Pairing effect and tensile properties of laminated high-performance hybrid composites prepared using carbon/glass and carbon/aramid fibers," *Composites Part B: Engineering*, vol. 79, pp. 61–6, 2015.
- [13] A. Monjon, P. Santos, S. Valvez, and PNB. Reis, "Hybridization effects on bending and interlaminar shear strength of composite laminates," *Materials (Basel)*, vol. 15, no.4, pp. 1–14, 2022.
- [14] Y. Swolfs, L. Gorbatikh, and I. Verpoest, "Fibre hybridisation in polymer composites: A review," *Composites Part A: Applied Science and Manufacturing*, vol. 67, pp. 181–200, 2014.
- [15] M.H. Ikbali, A. Ahmed, W. Qingtao, Z. Shuai, and L. Wei, "Hybrid composites made of unidirectional T600S carbon and E-glass fabrics under quasi-static loading," *Journal of Industrial Textiles*, vol. 46, no. 7, pp. 1511–35, 2017.
- [16] W. Wu, Q. Wang, A. Ichenihi, Y. Shen, and W. Li, "The effects of hybridization on the flexural performances of carbon/glass interlayer and intralayer composites," *Polymers (Basel)*, vol. 10, 5, p. 549, 2018.
- [17] W. Wu, Q. Ang, and W. Li, "Comparison of tensile and compressive properties of carbon/glass interlayer and intralayer hybrid composites," *Materials (Basel)*, vol. 11, no. 7, 2018.

- [18] R. Guo, G. Xian, C. Li, X. Huang, and M. Xin, "Effect of fiber hybridization types on the mechanical properties of carbon/glass fiber reinforced polymer composite rod," *Mechanics of Advanced Materials and Structures*, vol. 0, no. 0, pp. 1–13, 2021.
- [19] G. Agarwal, A. Patnaik, and J. Agarwal, "Effect of stacking sequence on physical, mechanical and tribological properties of glass-carbon hybrid composites," *Friction*, vol. 2, no. 4, pp. 354–64, 2014.
- [20] N.V. Pujar, N.V. Nanjundaradhya, and R.S. Sharma, "Experimental studies on the tensile and flexural properties of epoxy based unidirectional glass/carbon interlayer hybrid composites," *AIP Conference Proceedings. AIP Publishing LLC*, p. 20041, 2019.
- [21] A.F. Abd Ghani, and J. Mahmud, "Characterisation of hybrid carbon glass fiber reinforced polymer (C/GFRP) of balanced cross ply and quasi isotropic under tensile and flexural loading," *International Journal of Automotive and Mechanical Engineering*, vol. 17, no. 1, pp. 7792–804, 2020.
- [22] D. Matykiewicz, "Hybrid epoxy composites with both powder and fiber filler: a review of mechanical and thermomechanical properties," *Materials (Basel)*, vol. 13, no. 8, p. 1802, 2020.
- [23] S. Halder, P.K. Ghosh, M.S. Goyat, and S. Ray, "Ultrasonic dual mode mixing and its effect on tensile properties of SiO<sub>2</sub>-epoxy nanocomposite," *Journal of Adhesion Science and Technology*, vol. 27, no. 2, pp. 111–24, 2013.
- [24] P.K. Ghosh, K. Kumar, and N. Chaudhary, "Influence of ultrasonic dual mixing on thermal and tensile properties of MWCNTs-epoxy composite," *Composites Part B: Engineering*, vol. 77, pp. 139–44, 2015.
- [25] A. Mohanty, and V.K. Srivastava, "Effect of alumina nanoparticles on the enhancement of impact and flexural properties of the short glass/carbon fiber reinforced epoxy based composites," *Fibers and Polymers*, vol. 16, no. 1, pp. 188–95, 2015.
- [26] A. Afrouzian, H. Movahhedi Aleni, G. Liaghat, and H. Ahmadi, "Effect of nano-particles on the tensile, flexural and perforation properties of the glass/epoxy composites," *Journal of Reinforced Plastics and Composites*, vol. 36, no. 12, pp. 900–16, 2017.
- [27] H.B. Kaybal, H. Ulus, O. Demir, ÖS Şahin, and A. Avcı, "Effects of alumina nanoparticles on dynamic impact responses of carbon fiber reinforced epoxy matrix nanocomposites," *Engineering Science and Technology, an International Journal*, vol. 21, no. 3, pp. 399–407, 2018.
- [28] M. Abu-Okail, N.A. Alsaleh, W.M. Farouk, A. Elsheikh, A. Abu-Oqail, YA. Abdelraouf, et al. "Effect of dispersion of alumina nanoparticles and graphene nanoplatelets on microstructural and mechanical characteristics of hybrid carbon/glass fibers reinforced polymer composite," *Journal of Materials Research and Technology*, vol. 14, August, pp. 2624–37, 2021.
- [29] A. Goren, and C. Atas, "Manufacturing of polymer matrix composites using vacuum assisted resin infusion molding," *Archives of Materials Science and Engineering*, vol. 34, no. 2, pp. 117–20, 2008.
- [30] ASTM International, "Standard test method for tensile properties of polymer matrix composite materials," ASTM D3039, 2007.
- [31] ASTM International, "Standard test methods for flexural properties of unreinforced and reinforced plastics and electrical insulating materials," ASTM D790-07, 2007;
- [32] A.K. Kaw, *Mechanics of composite materials*. USA: CRC press, 2005.